Chapter 3

Substrate Integrated Waveguide Cavity Backed Wideband Slot Antenna for 5G Applications

3.1 Introduction

The fifth-generation (5G) is an mobile technology in order to meet the high data rate requirements, high bandwidth, improved security with shorter latency in coming years over 4G systems. The millimeter wave (mmWave) innovation is considered to be the most imaginative and effective solution among significant 5G technologies [137]. The technologies under 5G development includes massive multiple-input-multiple-output (MIMO), ultra-dense networking, dynamic spectrum sharing and full digital or hybrid beamforming [138,139]. It has been decided in World Radiocommunication Conference 2015 that operation of terrestrial International Mobile Telecommunications (IMT) services will take place within the frequency range between 24.25 to 86 GHz [140]. In this regard, 28 GHz frequency band (millimeter wave) has become a prominent candidate supporting high-speed communications (data rates up to 10 Gbps) along with large available bandwidth [141] and useful for non-line-of-sight communications.

Over the years, slot antennas have become one of the most popular choices among wireless communication systems due to their attractive advantages such as low profile, conformability, better isolation to feed network, easy integration, etc [142]. The slot antenna embedded in a metallic ground plane transmits in both directions, producing a bidirectional radiation pattern. This restricts the practical use of slot antennas in various situations. A good method to stop back radiation from slot antennas is to combine the antenna with a metal space behind the slot [143]. However, traditional cavity-backed slot antennas have high profiles, making integration with planar circuitry challenging. Recently, the substrate integrated waveguide (SIW) structure has been added to the planar cavity-backed slot antenna, which makes it possible to solve the problem above. Due to the high Q characteristic of the SIW cavity, the impedance bandwidth (BW) of the SIW cavity-backed slot antenna is narrow. To enhance the impedance bandwidth (IBW) of the SIW cavity-backed slot antenna, the authors have designed an inset-fed rectangular microstrip patch antennas (MSPA) SIW antenna to operated at 28 GHz frequency band for 5G wireless communication systems. This rectangular patch antenna is drilled with arrays of metallic vias on its three sides thereby forming PEC walls and fourth side as PMC wall being devoid of any metallic via. All the simulations are performed using ANSYS Electronics Desktop ver. 18.0.

3.2 Design of the Proposed Antenna

3.2.1 Antenna Configuration

The configuration of the proposed antenna (both top and bottom view) is outlined in Fig. 3.1 which consists of an inset-fed rectangular patch antenna, an U-shaped slot in the ground plane and a SIW cavity created by the single row of the metallic cylindrical vias around the rectangular patch and inside the planar substrate thereby making the four sidewalls of the cavity. In Fig. 3.1, the metallic (or copper) part of the proposed

antenna are represented with yellow, substrate with light green and metallic vias with blue color. These metallic vias connect the ground plane and radiating patch with each other. The proposed antenna is designed on Rogers RT/Duroid 5880 substrate having permittivity ε_r=2.2 and thickness h=0.508 mm with extremely low loss tangent $tan\delta$=0.0009. Many closely and equally spaced cylindrical metallic vias are drilled into the substrate and metalized from inside, thus acting as a short between the rectangular patch and ground plane. The propagation of electromagnetic waves inside this SIW cavity resembles the propagation in artificial periodic waveguide thereby minimizing the leakage losses to adequate levels. If the vias are placed in such a way that they cut the flow of currents, then a large amount of radiation may appear. On the other hand, if the vias are placed in the direction of the current, then only a little or no radiation will take place. The presence of gaps between the vias does not allow the TM modes to exist within the SIW [29]. The overall physical dimensions of the proposed antenna are 18×14 mm^2. The main purpose of using the metalized vias forming the SIW cavity is to effectively suppress and effects of edge diffraction of surface waves propagating over the entire substrate and confine the energy beneath the radiating patch. In this way, this array of metalized vias will also improve the radiation performance (gain and directivity levels). For this, the via diameter should be large and the distance between the vias is kept as small as possible in order to minimize the leakage loss ($L_{leakage} = -10log[S_{11}^2 + S_{12}^2]$) between the adjacent vias [144]. The center-to-center distance between each via of diameter d_{via} is represented by p_{via}. Two conditions related to these two parameters for minimizing the radiation loss are given by [38]

$$\frac{p_{via}}{d_{via}} < 2 \tag{3.1a}$$

$$d_{via} < \frac{\lambda_g}{5} \tag{3.1b}$$

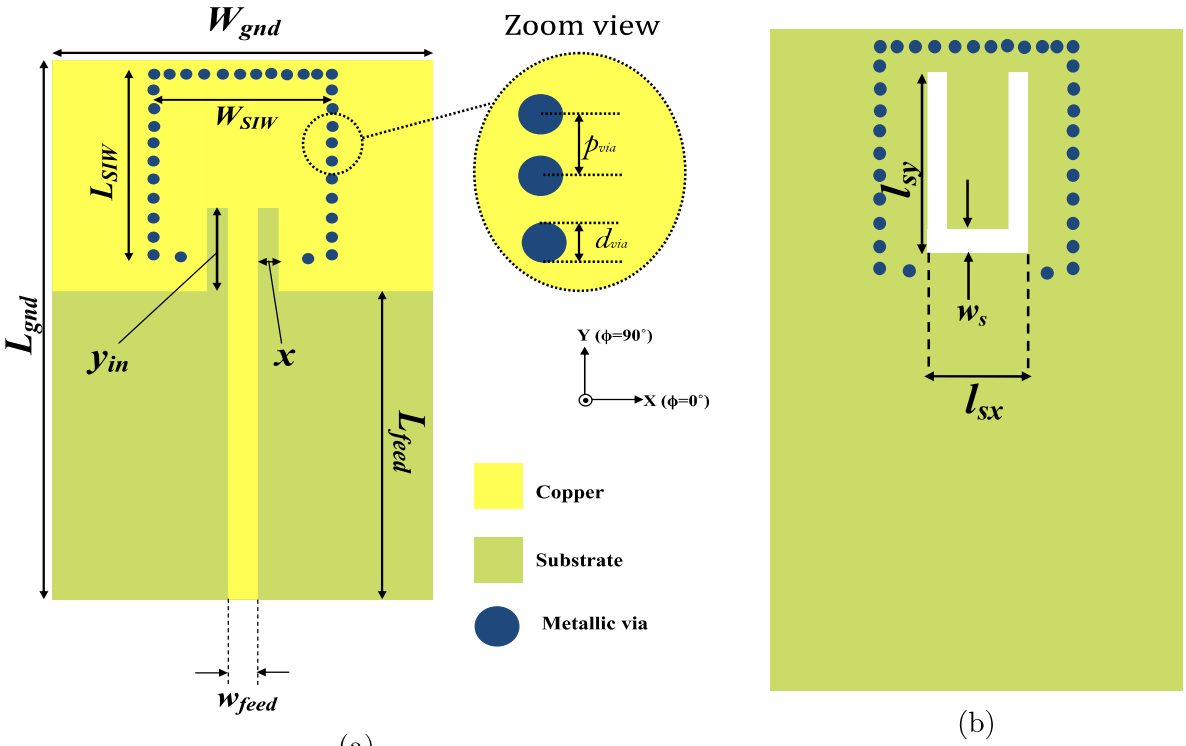

Figure 3.1: The geometrical configuration of the proposed antenna. (a) Top view (b) Bottom view. The detailed optimized dimension of the proposed SIW antenna are: L_{gnd}=18 mm, W_{gnd}=14 mm, L_{SIW}=6 mm, W_{SIW}=9 mm, d_{via}=0.4 mm, p_{via}=0.6 mm, w_{feed}=3.37 mm, L_{feed}=8 mm, y_{in}=5.5 mm, x=1.68 mm, l_{sy}=4.1 mm, l_{sx}=5 mm, w_s=1 mm.

The term W_{SIW} is the distance between the centers of two vias of opposite rows as shown in Fig. 3.1(a) and for dominant TE_{10} mode [145] is the guided wavelength corresponding to highest wavelength or lowest resonant frequency for 5G applications (which is around 26 GHz). Equations (4.1a-4.1b) ensure in keeping the leakage loss at negligible level. A rough estimate of cavity dimensions W_{SIW} and L_{SIW} (both are in millimeter) for a wideband antenna of bandwidth equals to $(f_H - f_L)$ (both are in GHz) can be calculated by [146]:

$$\lambda_g = \frac{2}{\sqrt{\frac{4f^2\varepsilon_r}{c^2} - (\frac{1}{W_{RWG}})^2}} \tag{3.2}$$

$$L_{SIW} \approx \frac{580.95}{\sqrt{\varepsilon_r}} \sqrt{\frac{1}{4f_H^2 - f_L^2}} \tag{3.3a}$$

$$W_{SIW} \approx \frac{580.95}{\sqrt{\varepsilon_r}} \sqrt{\frac{1}{4f_L^2 - f_H^2}} \tag{3.3b}$$

To cover the high frequency band of 5G completely, the upper (f_H) and lower (f_L) cutoff frequencies are taken as 26 GHz and 30 GHz, respectively. The relationship between the resonance frequency for any TE_{mnp} of the SIW cavity formed by the vias and geometrical parameters related to the proposed antenna dimensions can be given by following equation [147]:

$$f_{mnp} = \frac{1}{2\sqrt{\mu_o \varepsilon_o}} \sqrt{(\frac{m}{L_{RWG}})^2 + (\frac{n}{W_{RWG}})^2 + (\frac{n}{h})^2} \tag{3.4}$$

where

$$L_{RWG} = L_{SIW} - \frac{1.08 p_{via}^2}{d_{via}} + \frac{0.1 p_{via}^2}{L_{SIW}} \tag{3.5a}$$

$$W_{RWG} = W_{SIW} - \frac{1.08 p_{via}^2}{d_{via}} + \frac{0.1 p_{via}^2}{W_{SIW}} \tag{3.5b}$$

The terms m, n, p are the modal indices, L_{RWG} and W_{RWG} are the effective lengths and widths of the SIW cavity (equivalent to the rectangular waveguide), respectively. For obtaining more accurate values of L_{RWG} and W_{RWG}, following expressions can be considered:

$$W_{RWG} = W_{SIW}(\zeta_1 + \frac{\zeta_2}{\frac{p_{via}}{d_{via}} + \frac{\zeta_1 + \zeta_2 - \zeta_3}{\zeta_3 - \zeta_1}}) \tag{3.6a}$$

$$\zeta_1 = 1.0198 + \frac{0.3465}{\frac{W_{SIW}}{p_{via}} - 1.0684} \tag{3.6b}$$

$$\zeta_2 = -0.1183 - \frac{1.2729}{\frac{W_{SIW}}{p_{via}} - 1.2010} \tag{3.6c}$$

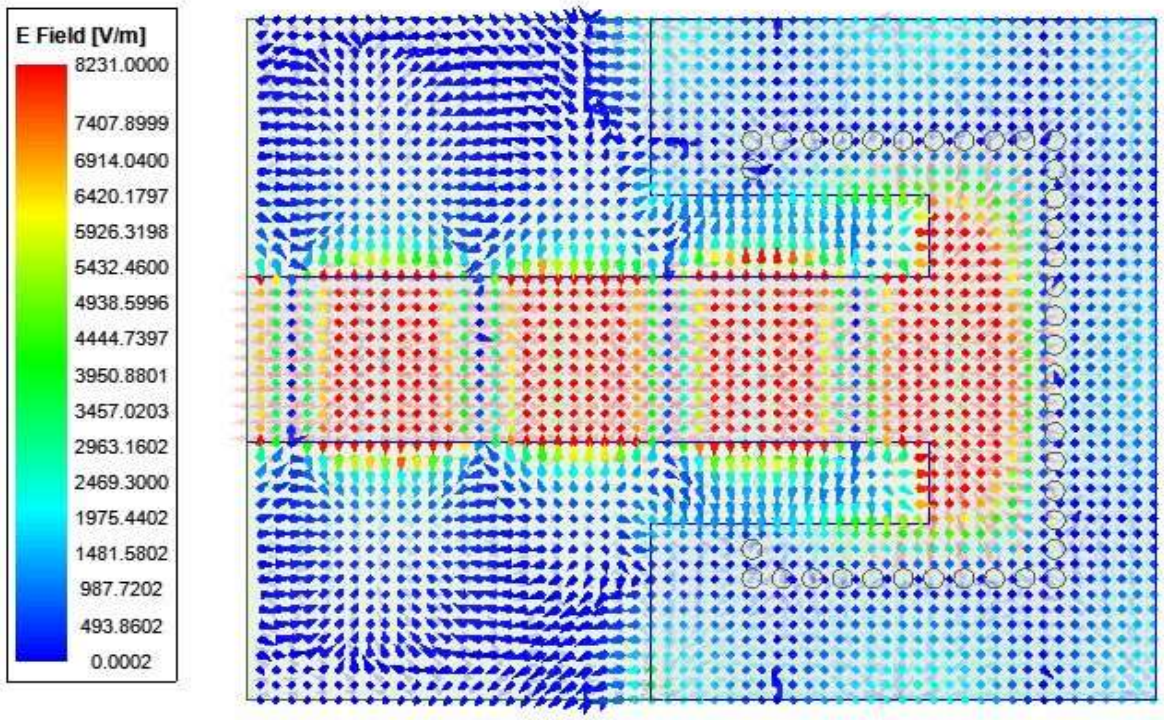

Figure 3.2: *E*-field distribution inside the SIW cavity.

$$\zeta_3 = 1.0082 - \frac{0.9163}{\frac{W_{SIW}}{p_{via}} + 0.2152} \tag{3.6d}$$

For W_{SIW}= 9 mm, p_{via}=0.6 mm and d_{via}=0.4 mm, the values of ζ_1, ζ_2, ζ_3 and W_{RWG} will be 1.05, -0.21, 0.95 and 8.69, respectively. Replacing W_{RWG} by L_{RWG} in equation (3.6a) gives L_{RWG} equals to 5.80 mm. The average value of the conductor losses (α_{ohmic}), dielectric losses (α_{diel}), radiation losses (α_{rad}) is computed by means of equations derived for the standard waveguide [36] are 2.80 dB, 2.50 dB, and 14.1 dB respectively within the range of operating frequency. The *E*-field distribution of the SIW cavity is shown in Fig. 3.2.

3.2.1.1 Patch Antenna and *U*-shaped Slot

Apart from the SIW cavity, the inset-fed MSPA can be designed using the following equations:

$$W_{patch}(= W_{gnd}) = \frac{c}{2f_r\sqrt{\frac{\varepsilon_r + 1}{2}}} \tag{3.7a}$$

$$L_{patch}(= L_{gnd} - L_{feed}) = \frac{c}{2f_r\sqrt{\varepsilon_{eff}}} - 2\Delta L \tag{3.7b}$$

where

$$\varepsilon_{eff} = \frac{\varepsilon_r + 1}{2} + \frac{\varepsilon_r - 1}{2\sqrt{1 + 12\frac{h}{W_{patch}}}}$$

and

$$\Delta L = 0.412h\frac{(\varepsilon_{eff} + 0.3)(\frac{W_{patch}}{h} + 0.264)}{(\varepsilon_{eff} - 0.258)(\frac{W_{patch}}{h} + 0.8)}$$

It is necessary to set the U-shaped slot dimensions at half-wavelength so as to get better radiation performance, i.e., gain and radiation efficiency levels. The relationship between the length of the slot and resonating frequency is given by:

$$f_{r,slot} \approx \frac{c}{2(2l_{sy} + l_{sx} - w_s)} \tag{3.8}$$

U-slot can be considered as a combination of three slots joined together in the form of a U-shape. Among these, two slots are of the arms of the U-slot l_{sy}, and these are in vertical form. The third one is the base of the U-slot l_{sx}, and it is in horizontal form. When the U-slot is incorporated into the ground plane, the resonance frequency will change due to the change in electrical size of the antenna. Now the current has to flow around the U-slot, and the length of the current path is increased on the edges, as shown in Fig. 3.3. It is clear from Fig. 3.3 that current density is maximum around

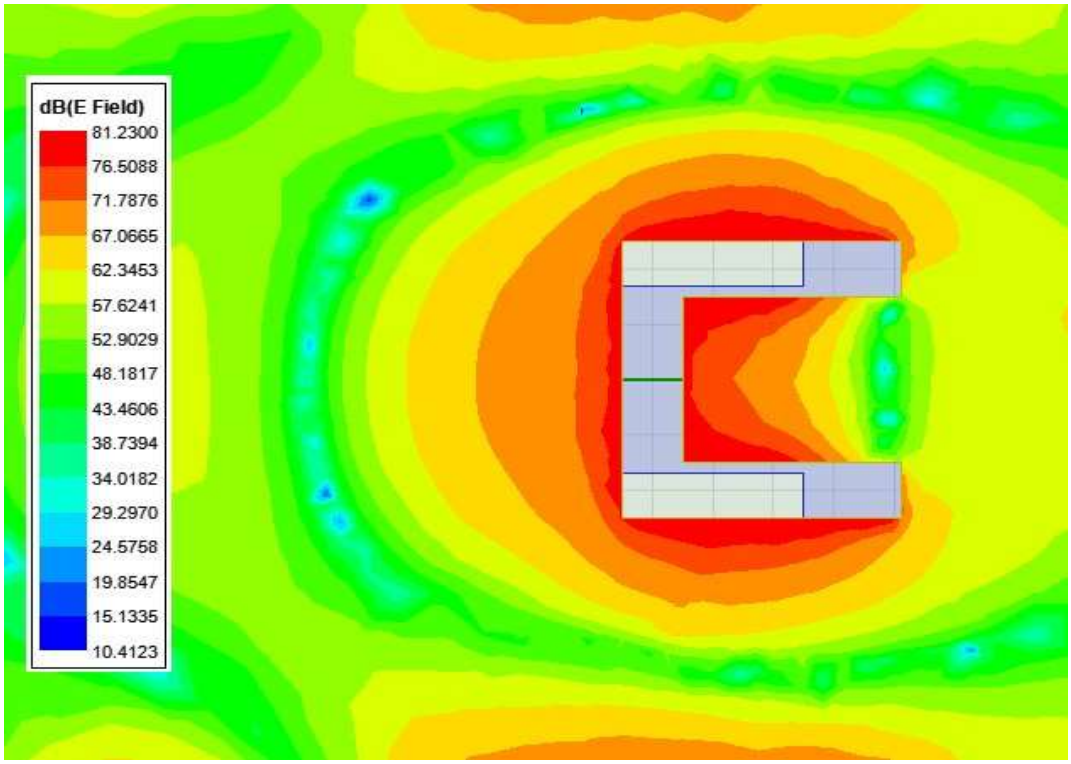

Figure 3.3: Surface current density around the U-shaped slot at $f_{r,slot}$=28 GHz.

the U-shaped slot at the resonating frequency.

3.3 Equivalent Circut Analysis

The equivalent circuit of the proposed SIW antenna (while ignoring the material losses) is shown in Fig. 3.4. Here, the presence of periodic vias decreases the overall permittivity of the substrate material used and hence suppresses the standing waves, resulting in the propagation of electromagnetic waves faster than in free space. To analyze the behaviour of the proposed cavity modes and their interaction with the slot antenna, the proposed design is analyszed with the help of an equivalent circuit model in ANSYS electronic desktop ver.18.0.

1. The equivalent circuit of the proposed antenna mainly consists of three branches, which show coupling of feed-line with mode-1, mode-2, and U-shaped slot.

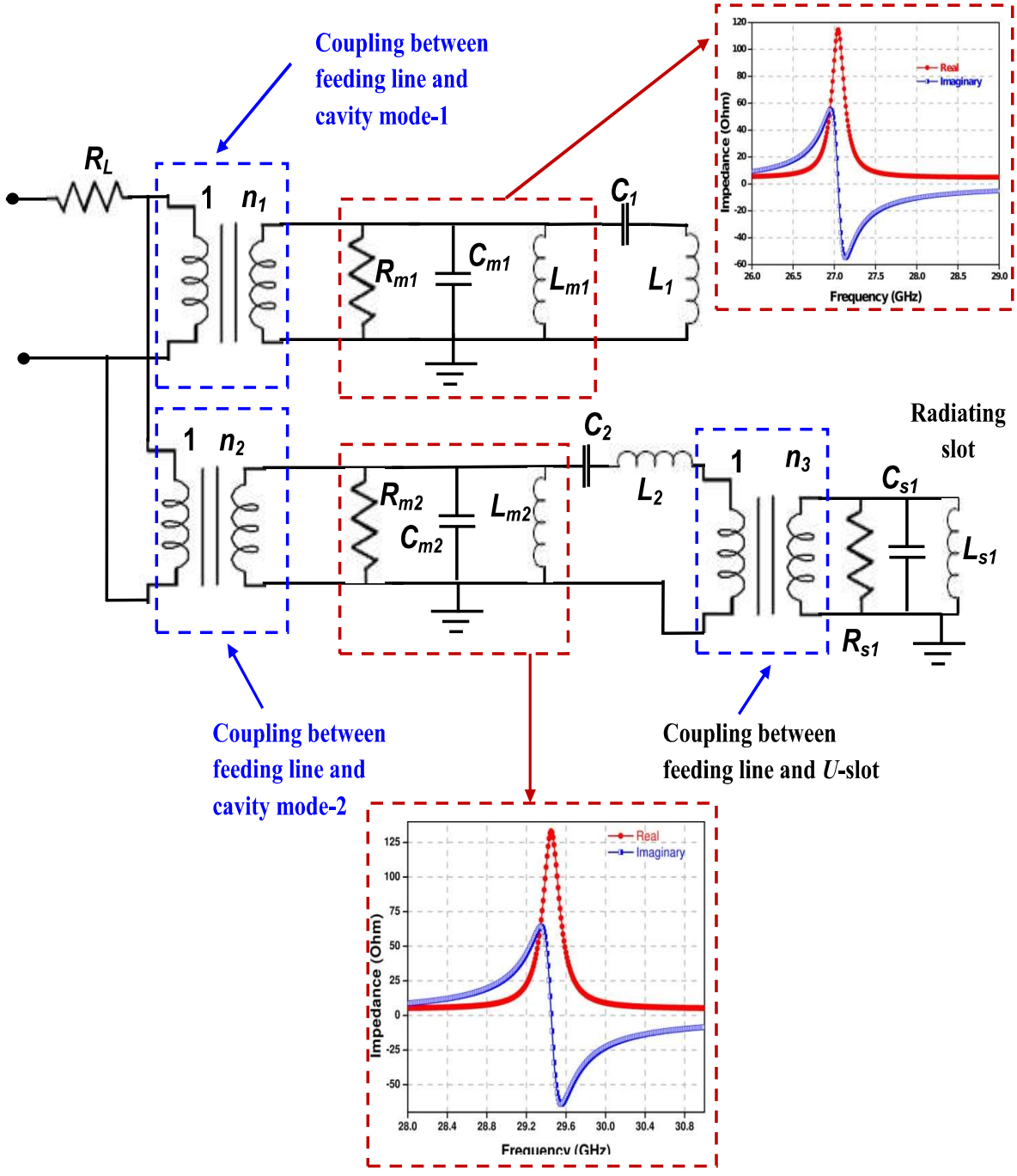

Figure 3.4: Final equivalent circuit of the proposed SIW antenna.

2. Here, the SIW cavity can be modelled as a parallel combination of RLC resonant circuits. The coupling between the feed-line and the propagating modes is represented with the help of an ideal transformer with turns-ratio 1:n. The optimized values of the circuit elements are as follows: R_L=4.68 Ω, n_1=25, R_{m1}=80.26 KΩ, C_{m1}=11fF, L_{m1}=3.148nH, R_{m2}=80.26 KΩ, L_{m2}=2.98 nH, C_{m2}=9.8 fF and n_2=27.
3. In order to widen the impedance bandwidth, U-shaped slot is etched in the ground plane of the proposed SIW antenna. The final equivalent circuit of the proposed SIW antenna considering both the propagating modes is shown in Fig. 3.4. Here, the combination of (R_{m1}, L_{m1} and C_{m1}) and (R_{m2}, L_{m2} and C_{m2}) corresponds to the cavity resonators which are coupled with the slot antenna with the help of transformers having turns-ratio n_1 and n_2, respectively. To model the effect of loading between two different cavity modes, a Tee network consisting of a series combination of a capacitor (C_1 or C_2) and an inductor (L_1 or L_2) is also placed with each arm. This capacitor-inductor series combination offer high impedance at the resonant frequencies and hence, a very small amount of signal is allowed to pass through them.

3.4 Parametric Analysis

In order to obtain the desired resonant frequency and matching characteristics over a specific range of frequency, parameterization over various parameters has been performed. While varying a particular parameter, all other parameters are kept constant. In this section, the effect of parameters, namely SIW cavity width, i.e., the center-to-center distance between the rows of the metallic vias and the arm length of U-shaped slot, has been studied. All the simulations related to parametric analysis have been performed using *Optimetrics* option given in the ANSYS Electronics Desktop version 18.0.

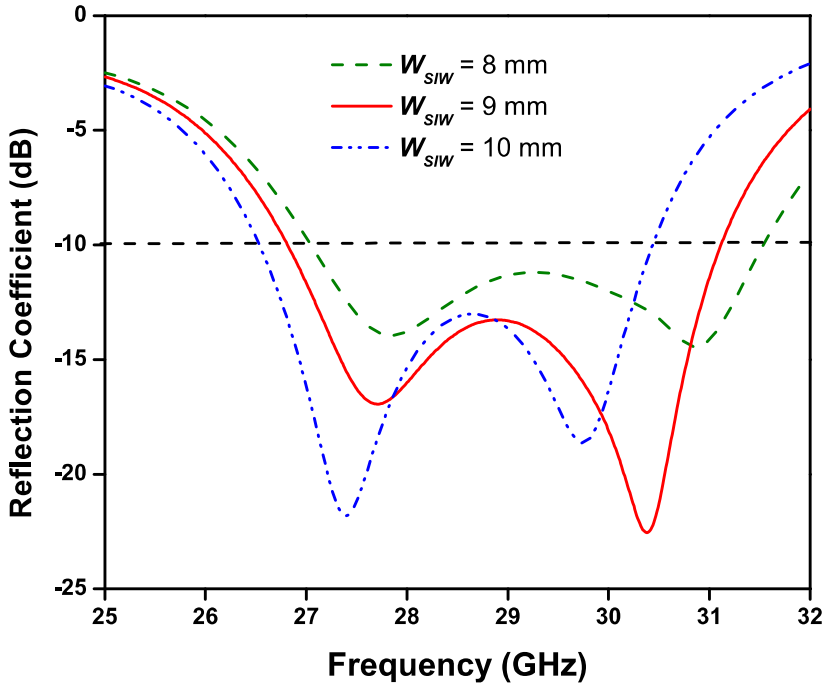

(a)

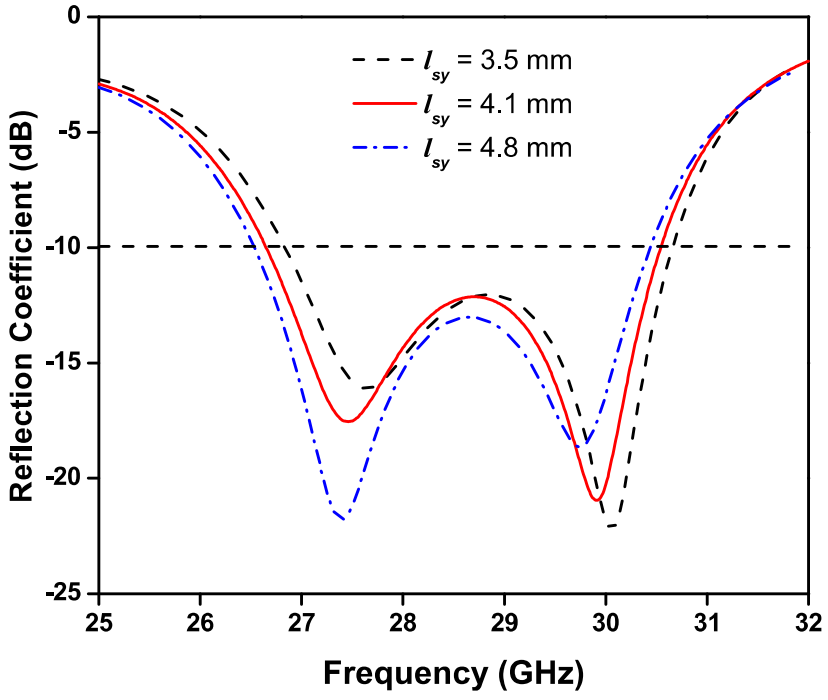

(b)

Figure 3.5: Variation in reflection coefficient (S_{11}) while varying (a) cavity width W_{SIW} and (b) arm lengths of U-shaped slot.

3.4.1 Influence of cavity width W_{SIW}

It is evident from equation (3.4) that any variation in the width of the SIW cavity brings variation in its resonating frequency. Fig. 3.5(a) shows the variation in matching characteristics with a change in W_{SIW}. As W_{SIW} varies from 8 mm to 10 mm, the upper cutoff frequency changes from 31.54 GHz to 30.44 GHz, i.e., by 3.49%. A very small or no effect on the lower resonating frequency has been noticed.

3.4.2 Influence of arm lengths of U slot

Though the W_{SIW} primarily determines the operating frequency of the antenna, however it can be modeled l_{sy} up to some extent. The presence of U-shaped slot in the ground plane decreases the quality factor and hence helps in improving the impedance bandwidth of the proposed SIW antenna. The effect of slot arm length l_{sy} is shown in Fig. 3.5(b). As the length l_{sy} increases, a longer effective current flows on the bottom surface of the cavity which reduces the resonating frequency (inverse relation). When the slot and cavity dimensions are in resonance, the energy will radiate into the space with utmost extent.

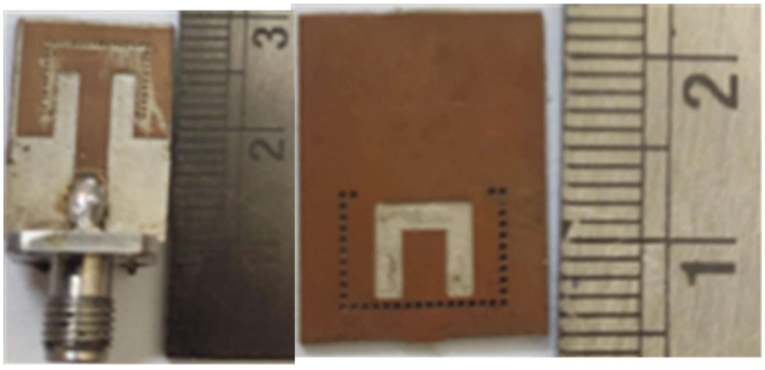

Figure 3.6: Photograph of the proposed antenna fabricated prototype.

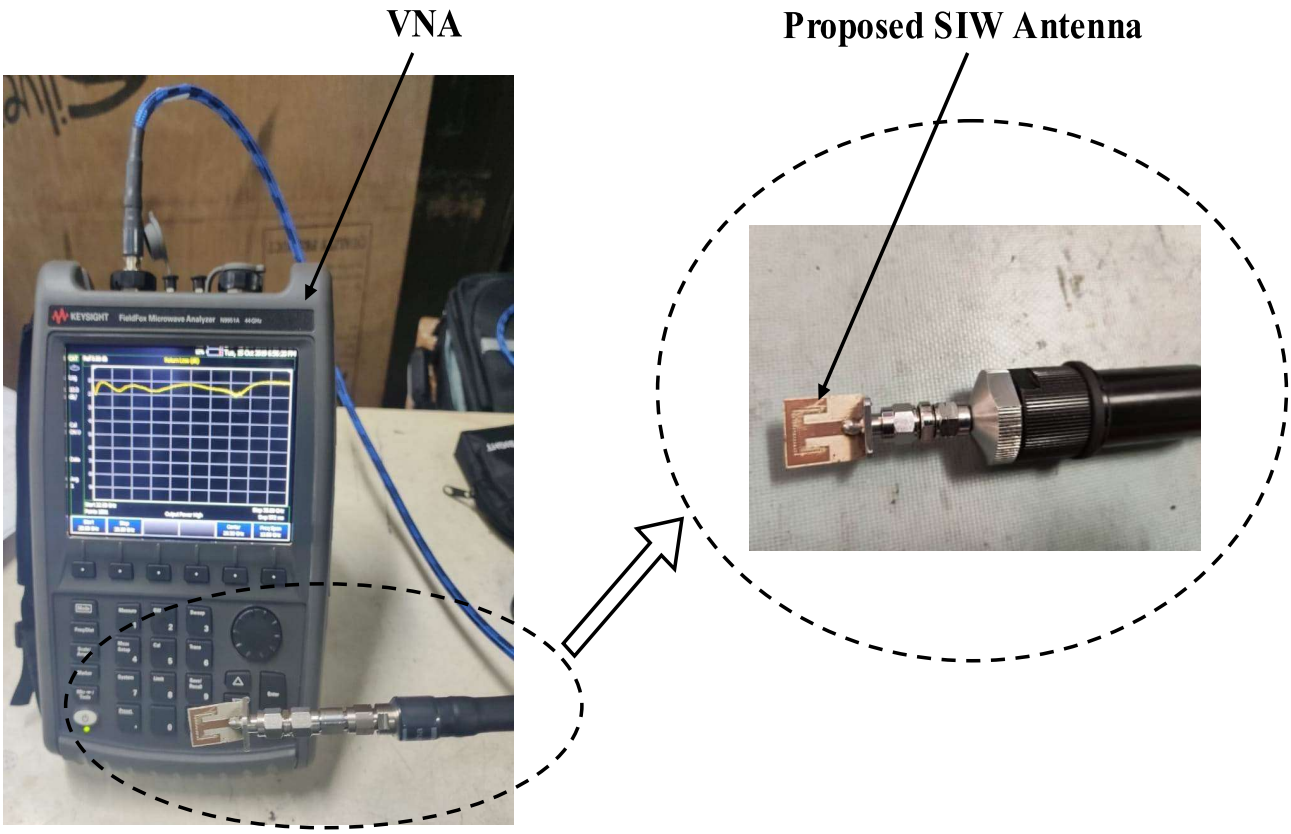

Figure 3.7: Testing of the proposed SIW antenna for measuring reflection coefficient using VNA.

3.5 Results and Discussion

3.5.1 Matching Characteristics

Fig. 3.6 shows the fabricated prototypes of the proposed SIW antenna having U-shaped slot in the ground plane. The proposed antenna is fabricated using standard PCB process and process of making vias inside the substrate material is explained in detail in [148]. The measurement of reflection coefficient (S_{11}) can be accomplished by using the Keysight N9951A FieldFox Microwave Analyzer as shown in Fig. 3.7. A 2.92mm(F) 4-hole panel mount 50Ω connector (can work up to 40 GHz) is connected to the proposed antenna for measurement purpose. Fig. 3.8 shows the simulated and measured S_{11} for the proposed antenna having an impedance bandwidth of 14.51% (26.20-30.30 GHz)

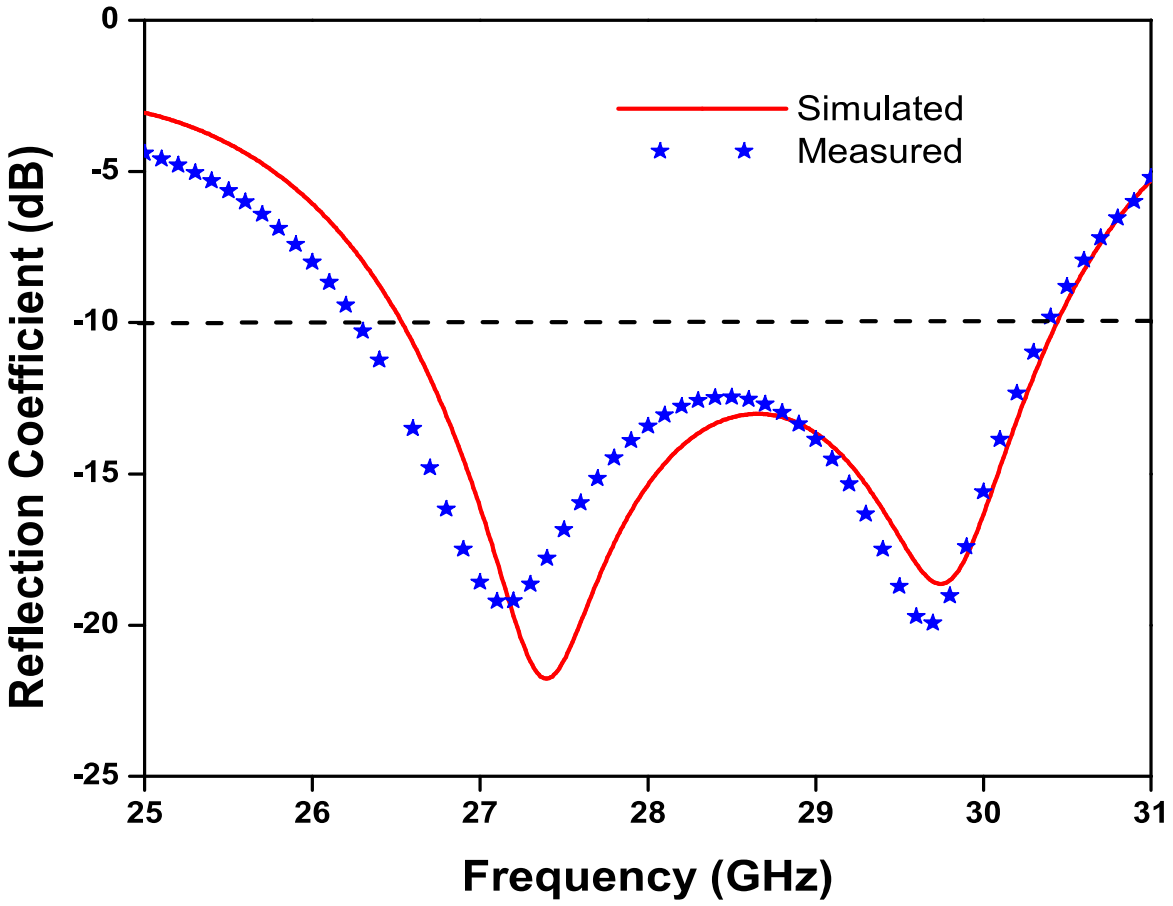

Figure 3.8: Simulated (solid red line) and measured (blue dotted line) reflection coefficient of the proposed antenna.

for $|S_{11}| \leq$ -10 dB. The proposed antenna design has been fabricated in a very careful manner. Also, the experimental results deviated from the simulated ones by less than $\pm$2.0% [149] throughout the work. Tolerances for simulated vs. experimental resonating frequencies of the proposed antenna are $\pm$0.73% for 27.1 GHz and $\pm$0.33% for 29.6 GHz. The proposed design achieves similar or better performance in bandwidth, with lower cost, lower sensitivity to fabrication tolerances. Hence, the proposed antenna is best suited for 5G application including 27.50-28.28 GHz in Japan, 26.50-29.50 GHz in Korea and 27.50-28.35 GHz in USA.

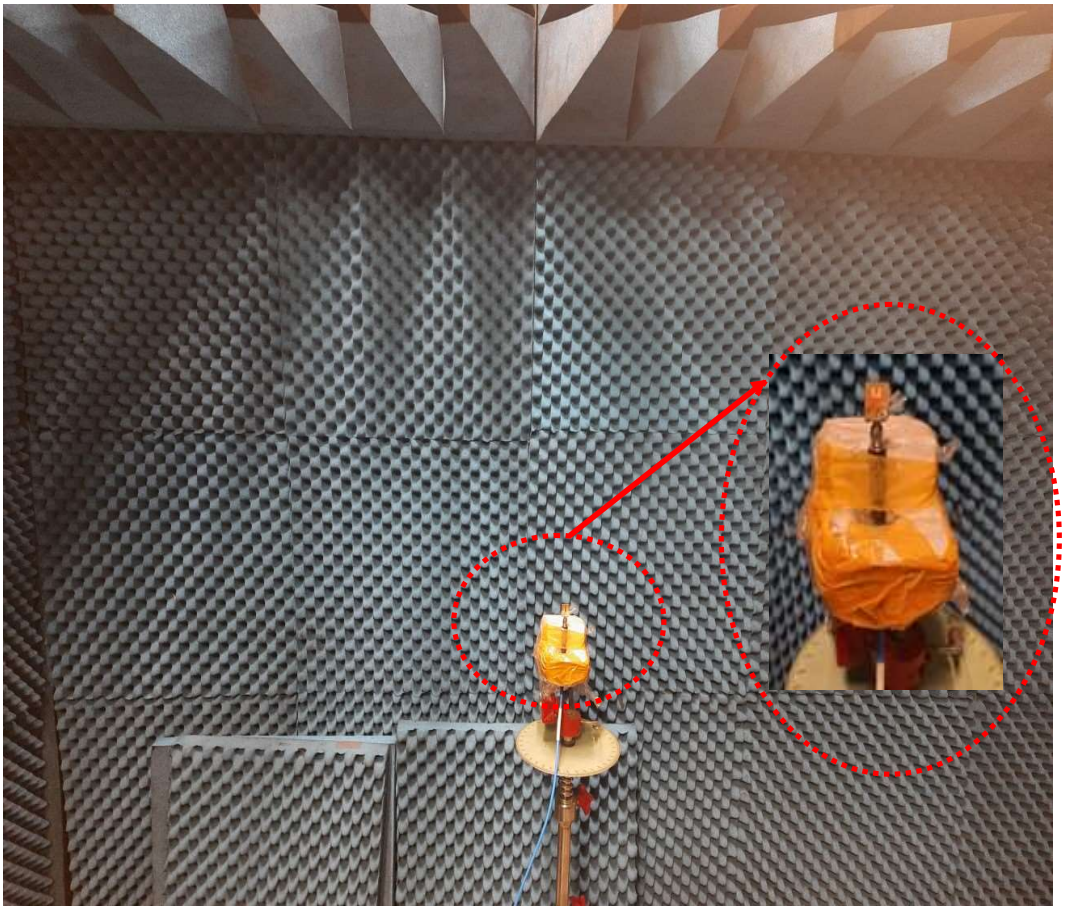

Figure 3.9: Proposed antenna placed inside anechoic chamber for the measurement of gain and radiation patterns.

3.5.2 Radiation Characteristics

All the measurement related to gain and efficiency are performed within the anechoic chamber as shown in Fig. 3.9. Fig. 3.10 shows the measured gain and radiation efficiency of the proposed antenna structure and a simple inset-fed antenna, i.e., without any SIW cavity and slot, respectively. It is clear that the presence of the SIW cavity and slot improves both gain and efficiency levels by minimizing the losses as compared to a simple MSPA having none of them. A maximum gain of 7.65 dBi at 28.5 GHz is obtained with variation less than $\pm$0.26 dBi within the operating frequency range. Also, the radiation efficiency of the proposed antenna is always larger than 90% with maximum of 91.29%

at 28.5 GHz and variation less than ±0.09% within the operating frequency range. The 1-dB gain bandwidth of the proposed antenna is 11.93% (26.80-30.20 GHz) and radiation efficiency within this range is larger than 90% which is about 8% better than the slotted SIW antenna reported in [150].

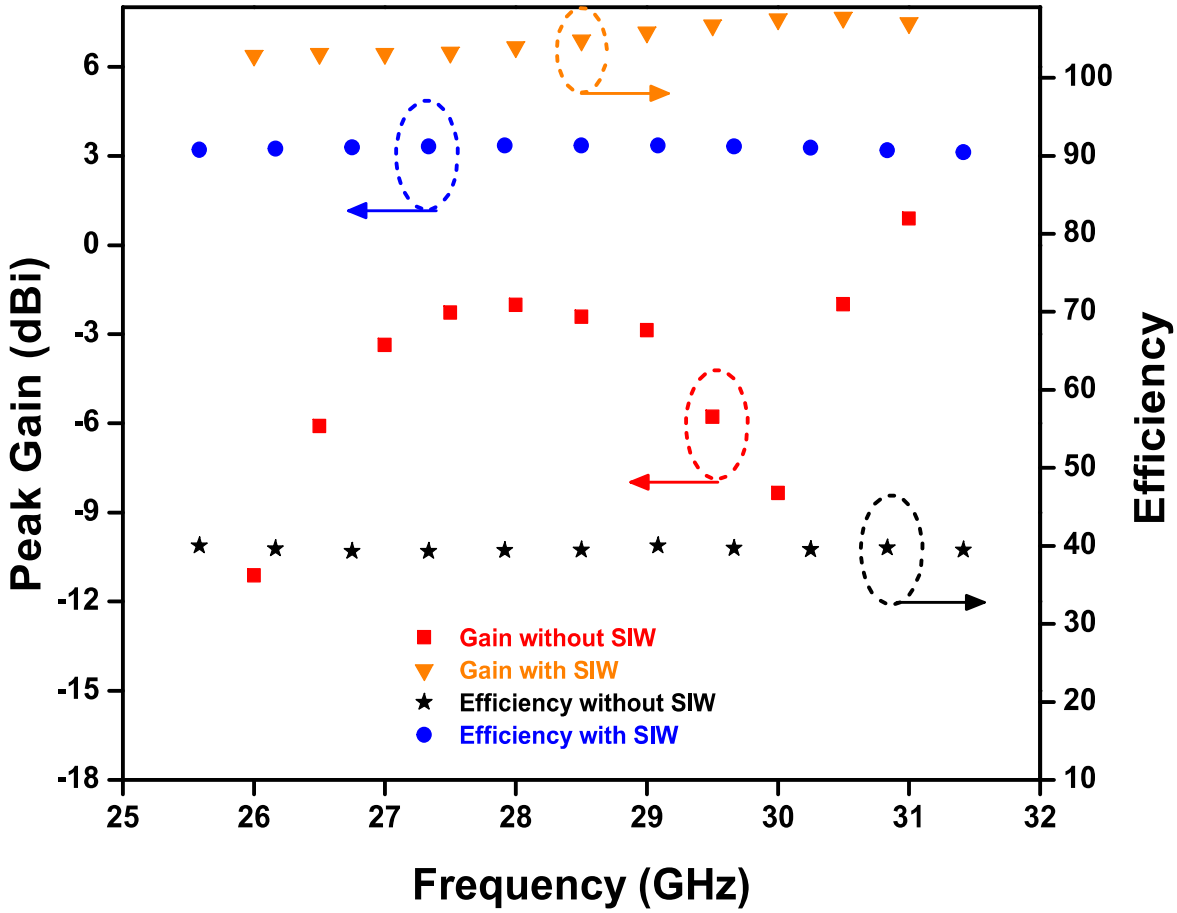

Figure 3.10: Gain and efficiency of the proposed antenna (without SIW cavity and slot).

The simulated and measured radiation patterns in XZ-plane (or ϕ=0°) and YZ-plane (or ϕ=90°) are illustrated in Fig. 3.11. The isolation level in XZ-plane and YZ-plane is about 28 dB and 35.4 dB, respectively at 27.1 GHz whereas the isolation level in XZ-plane and YZ–plane is less than 30 dB and 38 dB, respectively at 29.6 GHz. The mismatch between the simulation results and measurement results can be observed due to the misalignment between the fabricated proposed SIW antenna and the horn an-

tenna (of known gain) inside the anechoic chamber while performing the measurement. A comparison of the proposed antenna with the already proposed antenna structures is given in Table 3.1.

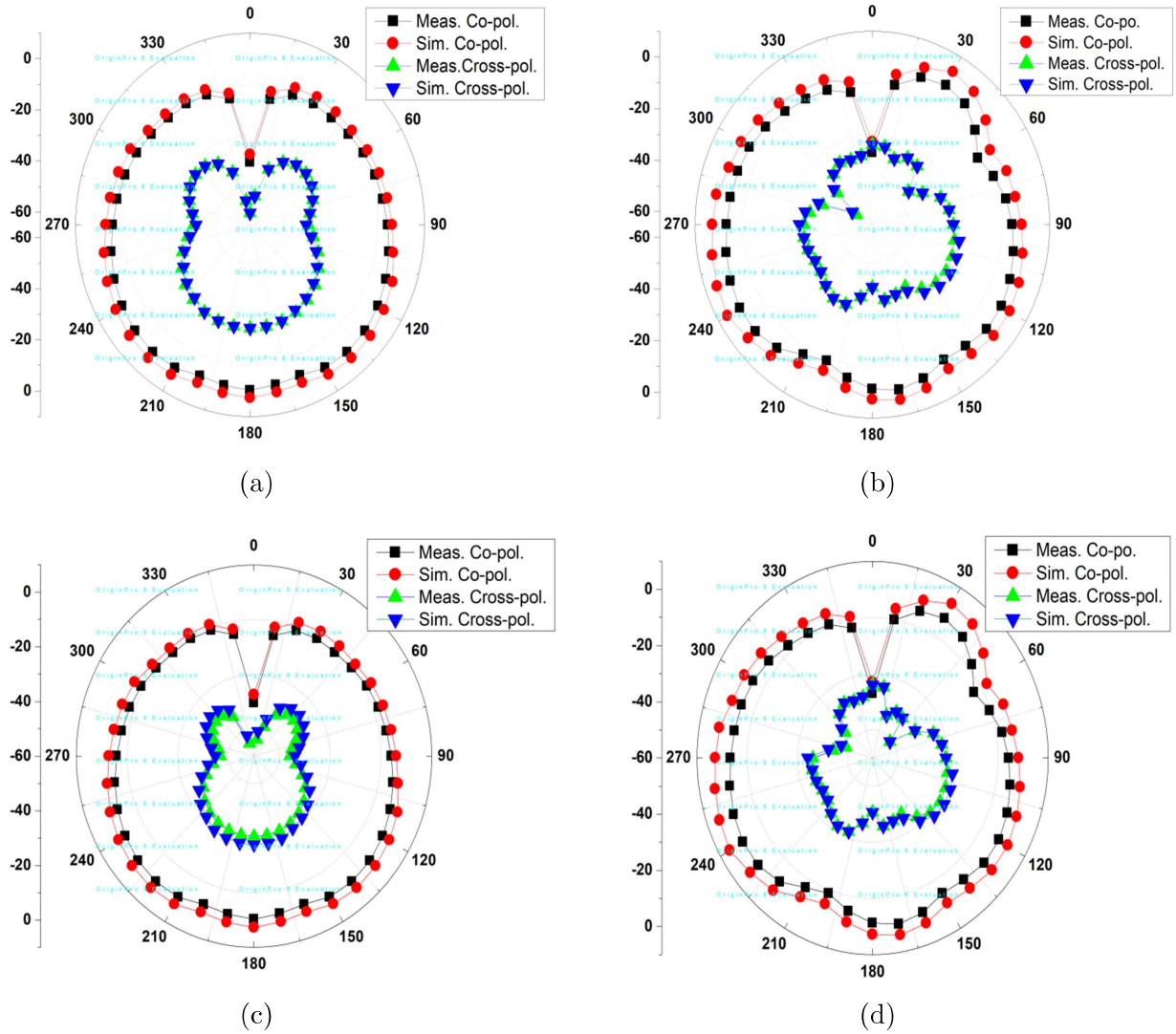

Figure 3.11: (a), (c) XZ plane (or ϕ=0°) and (b), (d) YZ plane (or ϕ=90°) normalized radiation pattern at 27.10 GHz and 29.60 GHz, respectively.

A wideband SIW cavity-backed slotted antenna is proposed and discussed in this chapter. The U-shaped slot is used to perturb the field distribution of the SIW cavity and helps in achieving a wideband response. The proposed antenna in presence of SIW cavity and U-shaped slot together shows impedance bandwidth of about 14.50%

Table 3.1: Comparison of measured results of the proposed slotted SIW antenna with antennas proposed for 5G applications

Reference/Year	**Dimensions (mm^3)**	**Bandwidth (%)**	**Peak Gain (dBi)**	**Technology used**
[151]/2020	30×35×0.76	25.50-29.60 GHz (14.88%)	8.3	Defected ground structure (DGS) MIMO
[152]/2019	38.58×38.58×0.762	27-29.20 GHz (7.83%)	12	Bow-tie antenna with DGS
[153]/2020	-	27.50-28.35 GHz (3.04%)	11	Rotated wide-slot
[154]/2018	11×31×0.254	26-31 GHz (17.54%)	10	Metamaterial based
[155]/2018	-	24.50-26.50 GHz (7.84%)	≥6	Aperture-fed + reconfigurable
[156]/2020	45×36×(0.787+0.65)	27.90-28.50 GHz (2.13%)	6.8	Multilayer configuration
Proposed Work	**18×14×0.508**	**26.20-30.30 GHz (14.51%)**	**7.65**	**SIW**

ranging from 26.20-30.30 GHz along with maximum peak gain and efficiency of 7.65 dBi and 91.29%, respectively. As compared to the conventional counterpart having no cavity and slot, the proposed antenna shows better gain and efficiency average levels by 11.09 dBi and 51.42%, respectively within the operating freqeuncy range. The parametric study of cavity and slot dimensions reveals their effect on antenna matching and resonance characteristics. The measured results of the proposed fabricated antenna prototype are in concordance with the simulated proposed antenna design. Due to its simple structure, high gain/efficiency levels and good radiation patterns, the proposed antenna can be an alternative for 5G and other wireless applications (including 27.50-28.28 GHz in Japan, 26.50-29.50 GHz in Korea and 27.50-28.35 GHz in USA).

The majority of the presented works in the literature are either multiple substrate-layered or use additional filtering structures at different layers for better isolation and do not emphasise the independent frequency tunability aspect of the design and require a smaller number of tuning parameters to be explored. So, there is a scope to design SIW-based planar, single substrate-layered self-diplexing and self-triplexing antennas having independent frequency tunability, which will be presented in the next chapter.